Adiabatic and approximate diabatic potential energy surfaces for the B...H2 van der Waals molecule

Millard H. Alexander

Citation: The Journal of Chemical Physics **99**, 6014 (1993); doi: 10.1063/1.465900
View online: http://dx.doi.org/10.1063/1.465900
View Table of Contents: http://scitation.aip.org/content/aip/journal/jcp/99/8?ver=pdfcov
Published by the AIP Publishing

Adiabatic and approximate diabatic potential energy surfaces for the B···H_2 van der Waals molecule

Millard H. Alexander
Department of Chemistry and Biochemistry, University of Maryland, College Park, Maryland 20742

(Received 30 April 1993; accepted 7 July 1993)

We report multireference configuration-interaction calculations for the lowest potential energy surfaces of the B($2s^2 2p\ ^2P$)···H_2 van der Waals molecule. The degeneracy of the $2p$ orbital implies that there exist *three* adiabatic potential energy surfaces (two of A' symmetry and one of A'' symmetry in C_s geometry) which become degenerate at large B–H_2 separation. By assuming that the two adiabatic states of A' symmetry correspond primarily to an orthogonal transformation of the in-plane B $2p$ orbitals, one can use calculated matrix elements of the electronic orbital angular momentum to transform to an approximate diabatic representation, which involves *four* potential energy functions. The proper angular expansion of these functions in terms of reduced rotation matrix elements is discussed and an analytic representation of the calculated points is obtained. The minimum energy of the B($2s^2 2p\ ^2P$)···H_2 van der Waals molecule is predicted to occur in C_{2v} geometry with an electronic symmetry of $^2B_2$, at a B–H_2 distance of 3.11 Å, and a dissociation energy D_e of 121 cm^{-1}. For the interaction of B(^2P) with p-H_2, assumed spherical in $j=0$, the zero-point corrected dissociation energy is $D_0=25$ cm^{-1}.

I. INTRODUCTION

As a consequence of the small bond dissociation energies of the metal hydrides,[1] the reaction of ground state metal atoms with hydrogen

$$M+H_2 \rightarrow MH+H \qquad (1)$$

is endothermic for all metals. In contrast, the electronic excited states are reactive, and there has been considerable experimental interest in such reactions.[2,3] One such study has involved initiation of reaction (1) from the M···H_2 van der Waals complex.[4] Concurrently, there has been some theoretical interest in these van der Waals complexes, in particular Li···H_2,[5] Mg···H_2,[6,7] and Cd···H_2.[8] Motivated by the ongoing experimental work on reactions of electronically excited B with H_2,[9] and on the spectroscopy of B in molecular hydrogen matrices,[10] we have undertaken the *ab initio* determination of the potential energy surfaces which are accessed by the approach to H_2 to B in its ground ($2s^2 2p\ ^2P$) electronic state.

The complicating, and challenging, feature of the B···H_2 system, as compared to the interaction of an S-state atom [Li($2s$) or Mg($3s^2$)] with H_2, is the additional complexity introduced by the threefold degeneracy of the $2p$ orbital. In this respect, the B···H_2 system is analogous to the interaction of H_2 with ground-state C^+($2s^2 2p\ ^2P$), F($2s^2 2p^5\ ^2P$), or C($2s^2 2p^2\ ^3P$) or with electronically excited Na($3p\ ^2P$), Be($2s2p\ ^3P$) or Mg($3s3p\ ^{1,3}P$). Some years ago Rebentrost and Lester[11–13] carried out a pioneering study of the interaction of F($2s^2 2p^5\ ^2P$) with H_2, which included self-consistent field (SCF) calculations of the adiabatic potential energy surfaces,[11] transformation to an approximate diabatic basis,[12] and calculation of inelastic scattering cross sections.[13] Flower and Launay reported a similar study, but concentrating on collisions only with H_2 in its lowest rotational level.[14,15] Extensive generalized valence-bond (GVB) *ab initio* calculations on C(^3P)+H_2 have been reported by Dunning and Harding.[16] Less sophisticated calculations on Be(^3P)+H_2 have been carried out by Menzinger and coworkers.[17]

Hertel has given a general overview of the Na($3p\ ^2P$)+H_2 system.[18] Botschwina and co-workers have reported restricted Hartree–Fock (RHF)-SCF and CEPA calculations of the relevant adiabatic potential energy surfaces.[19] An algorithm proposed by Werner and Meyer[20] was then used to transform into an approximate diabatic representation. More recently, Halvick and Truhlar have used a diatomics-in-molecules method to determine approximate diabatic potential energy surfaces for this system,[21] which were subsequently used in quantum scattering calculations.[22] Yarkony[23] has described the exact calculation of the relevant electronically nonadiabatic matrix elements along the crossing seams for the Na+H_2 system.

Simons and co-workers have used multiconfiguration and complete-active-space SCF methods to describe the potential energy surfaces for the interaction of Mg(^3P) (Ref. 6) and Cd($^{1,3}P$) (Ref. 7) with H_2 and, more recently, Rosenkranz[7] has used multireference, configuration-interaction techniques to map out large regions of the Mg($3s3p\ ^1P$)–H_2 potential energy surfaces.

In general, the interaction of an atom in a P electronic state with H_2 can be attractive if a singly filled p orbital lies parallel to the H_2 molecule and is thus able to interact with the unfilled σ^* antibonding H_2 orbital. On the other hand, the interaction will likely be repulsive if a singly or doubly filled p orbital points directly toward the H_2 molecule. (A good drawing is given in Fig. 1 of Ref. 19.) For example,[16] in C_{2v} geometry the $^3B_2$ state of C+H_2, in which the $2p_{a_1}$ and $2p_{b_2}$ orbitals are occupied, is *repulsive* at long range, despite eventually becoming the ground state of the methylene radical. Formation of CH_2 is facilitated by a curve crossing (allowed in C_s geometry) between the $^3B_2$

 0021-9606/93/99(8)/6014/13/$6.00

state and the $^3A_2$ state, which itself is attractive at long range, because the $2p_{a_1}$ orbital is unoccupied. For the approach of H_2 to Be($2s2p\ ^3P$), atom insertion without a barrier is allowed[17] on the $^3B_2$ surface, in which the $2p$ electron lies parallel (b_2 symmetry) to the H_2 σ^* orbital.

The BH_2 molecule is a well characterized species with a bent structure[24] (H–B–H angle 131°, BH distance 1.18 Å, molecular symmetry $^2A_1$). The B–H_2 binding energy is substantial (349 ± 65 kJ/mol).[25] Notwithstanding, in contrast to the interaction of C(^3P) and Be*(^3P) with H_2, there is a significant barrier to molecular formation, since the H_2 molecule must be significantly stretched before insertion of the B atom can occur. In addition, the electron occupancy of the lowest B···H_2 state of $^2A_1$ symmetry is $1a_1^2 2a_1^2 3a_1^2 4a_1$, where $3a_1$ designates the H_2 bonding orbital and $4a_1$, the B $2p_z$ orbital. However, the electron occupancy of the lowest $^2A_1$ state of BH_2 is $1a_1^2 2a_1^2 1b_2^2 4a_1$.[24] The existence of a barrier to insertion will be demonstrated below by complete-active-space, self-consistent-field calculations.

Consequently, approach of the B($2s^2 2p\ ^2P$) atom to H_2 can lead only to a weakly-bound van der Waals adduct. We describe in Sec. II multireference, configuration-interaction (MRCI) calculations of the *three* ($^2A_1$,$^2B_1$,$^2B_2$) B($2s^2 2p\ ^2P$) H_2 potential energy surfaces as a function of the Jacobi coordinates which describe the orientation of the B atom about a rigid H_2 molecule. Except in the two high symmetry geometries (C_{2v} and $C_{\infty v}$), the two states which are symmetric (A') with respect to reflection of the wave function in the triatomic plane, will represent, in the simplest picture, an orthogonal transformation of the two in-plane orientations of the B $2p$ orbital [B(...$2p_z\ ^2P$) H_2 and B(...$2p_x\ ^2P$) H_2]. In an eventual treatment of the dynamics of the B($2s^2 2p\ ^2P$)+H_2 system it is most convenient to consider a *diabatic* representation of the interaction potential, in which the three states are characterized by the three Cartesian orientations of the B $2p$ orbital with respect to the vector R which joins the atom to the center-of-mass of the H_2 molecule.

Transformation to an approximate diabatic representation, in which the three states correspond, nominally, to the three body-frame orientations of the B $2p$ orbital, can be achieved easily by determination of the matrix elements of the electronic orbital angular momentum L, as proposed originally for the F+H_2 system by Rebentrost and Lester.[12]

The *ab initio* calculations will be described in the next section. This is followed, in Sec. III, with the discussion of the transformation to an approximate diabatic representation. The expansion of the resulting diabatic potential energy functions, in terms of Legendre and associated Legendre polynomials, is discussed in Sec. IV. Section V then summarizes the simplifications which can be made if the interaction of B(^2P) with H_2 in its lowest rotational level can be modeled by the assumption of a spherical H_2 molecule. Finally, we close with a brief conclusion.

II. *AB INITIO* CALCULATIONS

As mentioned in the Introduction, a series of exploratory calculations were done to confirm the existence of a substantial barrier to formation of the BH_2 molecule for approach of ground state B atoms to H_2. As an atomic orbital basis we used the valence and first polarization shell orbitals from the averaged atomic natural orbital basis of Roos and co-workers[26] (14*s*9*p*4*d* contracted to 6*s*5*p*3*d* for B and 8*s*4*p* contracted to 4*s*3*p* for H), a total of 62 contracted Gaussian functions. With this basis set, complete-active-space, self-consistent-field (CASSCF) (Ref. 27) calculations were performed, with 7 electrons in a space (exclusive of the 1*s* orbital on B) of four a' and one a'' orbitals. This excludes the H_2 antibonding σ orbital. Unfortunately, over the full range of configuration space explored it was not possible to consistently include this orbital, which is, of course, essential for a proper description of the breaking of the H–H bond. Except for significantly stretched H–H bond distances, the next higher orbitals of a' symmetry ($5a'$ and $6a'$) were found to correspond to B $3p$ and $3d$ orbitals, which contribute significantly to the correlation of the $2s$ electrons. Since we did not want to extend the active space to include all of the $n=3$ shell of B, which would have been necessary for an even-handed description of the three states of BH_2, we limited the active space to four a' and one a'' orbitals. All calculations were carried out with the MOLPRO suite of *ab initio* programs.[28]

To explore, and subsequently visualize, the barrier to formation of BH_2 accompanying approach of B to H_2 we chose a geometry which allowed the B atom to come in along a ray, oriented at a fixed angle with respect to the perpendicular bisector of the H_2 bond, as illustrated in the upper panel of Fig. 1. All of these rays were further located so as to intersect the position of the B atom at the equilibrium geometry of the ground state of the BH_2 molecule. This ensures that every two-dimensional plot of the potential energy surfaces as a function of the H–H distance and the length of the ray will include the equilibrium position of the BH_2 molecule. In total, calculations were performed at 1160 points. Figure 2 presents contour plots of the lowest BH_2 potential energy surface of A' symmetry for several different values of the orientation of the approach ray.

As can be seen clearly, approach on the $2^2A'$ surface (right-hand panels) is steeply repulsive. Clearly, all approaches to the molecular minimum involve passage over a high barrier. This barrier is an avoided crossing indicative of the orbital rearrangement prior to formation of the BH_2 molecule discussed in the Introduction (the electron occupancy of the lowest $^2A_1$ state of B···H_2 is $1a_1^2 2a_1^2 3a_1^2 4a_1$ while that of BH_2 is[24] $1a_1^2 2a_1^2 1b_2^2 4a_1$). In looking at Fig. 2, the reader should remember that the equilibrium geometry of the BH_2 molecule in its ground ($^2A_1$) electronic state occurs at the point $\rho=0$, $r_{H_2} = 4.06$ bohr,[24] which is far beyond the lower right hand corner of the contour plots. The lower surface of A' symmetry, which corresponds in C_{2v} geometry to the lowest $^2B_2$ state of BH_2, is less repulsive as the atom approaches the molecule, since the electron occupancy of this state is nominally the same for both

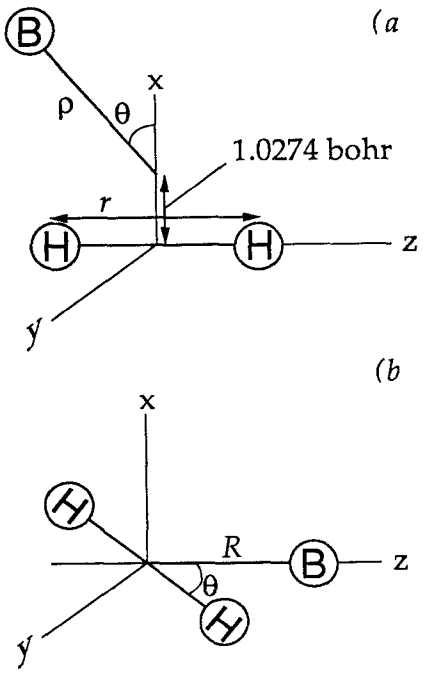

FIG. 1. (a) Coordinate system used for the study of the barriers to the formation of BH_2 from $B(^2P)+H_2$. The B atom is brought in along the ray ρ, which is oriented at a fixed angle θ with respect to the perpendicular bisector of the H_2 bond and which intersects the position of the B atom at the equilibrium geometry of the BH_2 molecule (Ref. 24). (b) Coordinate system used in the determination of the potential energy surfaces for the B···H_2 van der Waals molecule. The B atom is fixed along the z axis, and the H_2 molecule, constrained to its equilibrium bond distance of 1.402 bohr (as determined in our CEPA-1 calculations), is oriented in the xz plane at an angle θ with respect to the z axis.

the molecule and the van der Waals complex. Although a flattening and skewing of the potential energy surface occurs in a region of space roughly comparable to the barrier on the upper A' surface, the lower A' surface is monotonically repulsive, at least over the geometries explored here. Figure 2 displays results for approaches of the B atom at fixed orientations (Fig. 1) of 0°, 15°, and 30°. Calculations were also carried out for $\theta=45°$ and 60°. The behavior of the surfaces was qualitatively similar, and, for brevity, will not be shown here. In addition, the A'' surface (also not shown) is strongly repulsive. Here, too, the electron occupancy of the B···H_2 van der Waal's complex ($1a_1^2 2a_1^2 3a_1^2 1b_1$) differs from that of the lowest $^2B_1$ state of BH_2 ($1a_1^2 2a_1^2 1b_2^2 1b_1$) (Ref. 24).

Although no dynamic correlation effects were accounted for in these CASSCF calculations, the heights of the barriers is sufficiently large that we believe that even with the inclusion of dynamic correlation, molecule formation would not be possible for thermal velocities.

With this established, we proceeded to the exploration of the potential surfaces of the B···H_2 van der Waals molecule. A series of exploratory correlated electron pair (CEPA-1) (Refs. 29–31) calculations were performed in C_{2v} geometry to determine an appropriate atomic orbital basis set. We used the augmented correlation-consistent valence-triple-zeta (avtz) basis of Dunning and coworkers[32,33] (11*s*6*p*3*d*2*f* contracted to 5*s*4*p*3*d*2*f* for B and 6*s*3*p*2*d* contracted to 4*s*3*p*2*d* for H) as well as the *spdf* functions from the augmented correlation-consistent valence-quadruple-zeta (avqz) basis (13*s*7*p*4*d*3*f* contracted to 5*s*4*p*4*d*3*f* for B and 7*s*4*p*3*d* contracted to 5*s*4*p*3*d* for H). These avtz and avqz bases consisted, respectively, of a total of 92 and 126 contracted Gaussian functions. Further calculations were done using the averaged atomic natural orbital basis of Roos and co-workers[26] (14*s*9*p*4*d*3*f* contracted to 6*s*5*p*3*d*2*f* for B and 8*s*4*p*3*d* contracted to 4*s*3*p*2*d* for H). One additional diffuse function of each symmetry was added with exponents ($\zeta_s=0.008\,395$, $\zeta_p=0.016\,677$, $\zeta_d=0.051\,45$, and $\zeta_f=0.136$ for B and $\zeta_s=0.009\,787$, $\zeta_p=0.098\,827$, and $\zeta_d=0.291\,04$ for H). This basis, which we designate as *a-aano*, contained a total of 130 contracted functions. A still larger basis, *a-aano-g*, which contained 153 contracted functions, was obtained by adding to the *a-aano* basis a diffuse g function with exponent $\zeta=0.21$ on the B atom and a diffuse f function with exponent $\zeta=0.24$ on the H atoms.

In C_{2v} geometry each orientation of the B $2p$ orbital belongs to a different point group. The interaction energy for each orientation (a_1, b_1, and b_2) can be defined as

$$V(R)=E_{B\text{-}H_2}(R)-E_{H_2}(R)-E_B(R). \tag{2}$$

Since the CEPA calculations are size-consistent, no correction need be made for any residual size consistency of the calculations, which we define for future reference, as

$$\Delta E_{SC}=E_{B\text{-}H_2}(\infty)-E_{H_2}(\infty)-E_B(\infty). \tag{3}$$

The counterpoise correction, which is a measure of the degree of saturation of the atomic orbital basis, is defined as[34]

$$\Delta E_{CP}(R)=E_{H_2}(\infty)+E_B(\infty)-E_{H_2}(R)-E_B(R). \tag{4}$$

The upper panel of Fig. 3 displays the calculated interaction energies for C_{2v} B···H_2. As might be anticipated from Fig. 2, the $^2A_1$ potential is most repulsive, since for this orientation the B $2p$ orbital points directly at the H_2 bond and hence is most sensitive to Pauli repulsion with the filled (σ_g) H_2 bonding orbital. The $^2B_2$ potential is least repulsive. The b_2 orientation of the B $2p$ orbital allows the most favorable interaction between the quadrupole moment of the P-state B atom (with polarity *negative* at the ends of the two p lobes and *positive* at the nucleus) and the H_2 quadrupole (with polarity positive at the ends and negative in the middle), as well as the most favorable orientation of the axes of greatest polarizability of the both B and H_2. In addition, in this orientation the B $2p$ orbital avoids Fermi repulsion with the filled H_2 σ_g orbital. For all these reasons the van der Waals well is deepest for the $^2B_2$ state.

We observe that the avtz basis, which was the smallest basis used, yields interaction potentials which are virtually identical to those determined with the larger basis sets. Consequently, the avtz basis was used in our calculations of the full potential, in C_s geometry. CASSCF (Ref. 27)

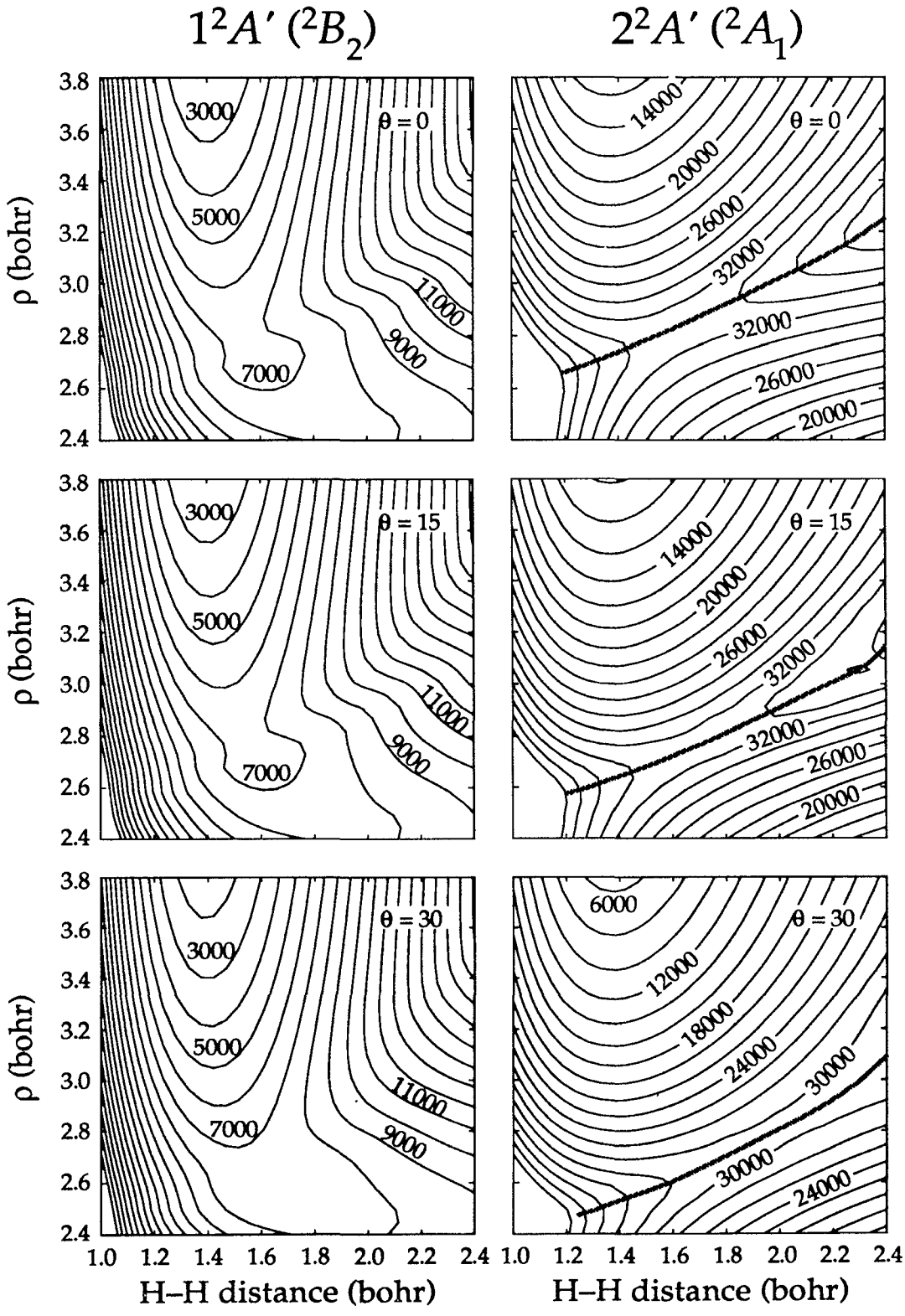

FIG. 2. Contour plots of the lowest CASSCF B(^2P)···H_2 potential energy surfaces of A' symmetry as a function of the H–H bond distance r and the distance ρ of the B-atom from its position at the equilibrium geometry of the BH_2 molecule; see Fig. 1. The orientation of ρ with respect to the perpendicular bisector of the H_2 molecule is, for the top to bottom panels, respectively, 0°, 15°, and 30°. The left-hand panels, with contours every 1000 cm^{-1}, depict the lower $1A'$ potential energy surface. In C_{2v} symmetry (top panel) this corresponds to the $^2B_2$ surface, in which the B $2p$ orbital is oriented *parallel* to the H_2 bond. The right-hand panels, with contours every 2000 cm^{-1}, depict the higher $2A'$ potential energy surface. In C_{2v} symmetry (top panel) this corresponds to the $^2A_1$ surface, in which the B $2p$ orbital is oriented *perpendicular* to the H_2 bond and in the triatomic plane. The barrier on the $2^2A'$ surfaces due to an avoided crossing is indicated by the thick gray contour. The equilibrium geometry of the BH_2 molecule occurs at the point $\rho=0$, r = 4.06 bohr, with $^2A_1$ symmetry.

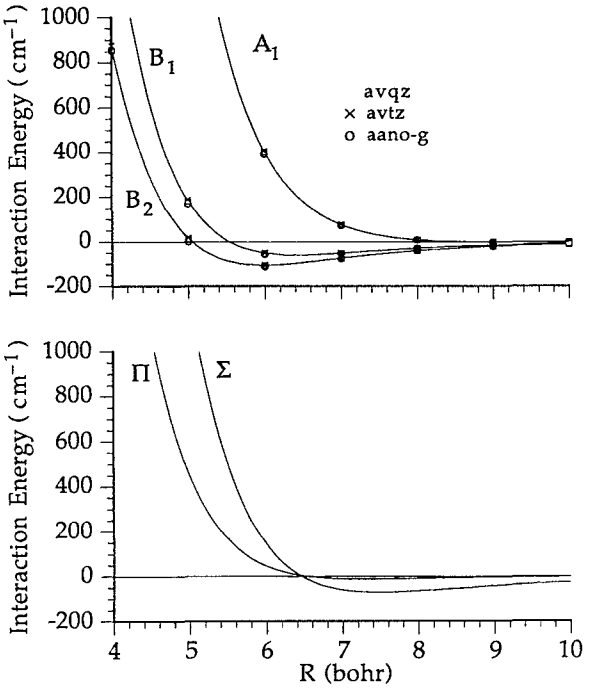

FIG. 3. (Upper) B(^2P)···H_2 CEPA-1 interaction potentials for C_{2v} geometry. The solid curves refer to calculations with the *a-aano* atomic orbital basis. The open circles, open squares, and crosses designate, respectively, the calculations with, respectively, the *a-aano-g*, avqz, and avtz bases. In every case the value of the H_2 bond distance was help fixed at 1.402 bohr. (Lower) B(^2P)···H_2 CEPA-1 interaction potentials for collinear geometry, determined with the *a-aano* atomic orbital basis.

calculations with 7 electrons in a space of $4a'$ and $1a''$ orbitals (with the exclusion of the 1*s* orbital of B and the σ^* orbital of H_2; see earlier in this section) were performed. State averaging,[20,35,36] with equal weighting, was used to obtain a single set of CASSCF orbitals for the $1A'$, $2A'$, and $1A''$ states. Subsequently, multireference, internally contracted, configuration-interaction calculations,[37] were carried out, in which only the 1*s* electrons of B were excluded. The effect of higher order excitations was estimated using the Davidson correction.[38]

Defining the B···H_2 Jacobi coordinates as shown in Fig. 2(b), we carried out MR-CI(D) calculations at B–H_2 angles θ of 1°, 5°, 15°, 30°, 45°, 60°, 75°, 85°, and 90°, and at 11 different values of the B···H_2 distance R (4, 4.5, 5, 5.5, 6, 6.5, 7, 7.5, 8, 9, and 10 bohr). No C_s symmetry calculations were done at the higher symmetry $D_{\infty h}$ geometries (θ=0°) to avoid convergence problems in the CASSCF or CI calculations due to root flipping. In all these calculations the H_2 bond length was maintained at 1.402 bohr, which corresponds to the equilibrium internuclear distance as determined with CEPA-1 calculations using the *a-aano* basis.

For C_s geometry it would be difficult to apply, in a consistent manner, a counterpoise correction to the calculated energies of the two states of A' symmetry, for the following reason: In general, as discussed above, the *upper*, more repulsive of the two A' surfaces will correspond to the B 2*p* orbital pointing toward the H_2 while the *lower* surface will correspond to an orthogonal, but in-plane, orientation of this orbital. However, in the counterpoise calculations for the B atom, the *lower* of the A' states will correspond to the 2*p* orbital pointing toward the H_2 molecule, since it is in this orientation that the empty H_2 orbitals can be used to greatest advantage by the B atom. Thus, it is difficult to predict, independent of geometry, which of the two B atom A' energies should be used in the counterpoise correction for a given BH_2 state of A' symmetry.

This ambiguity could be resolved by transformation of the adiabatic energies of the two A' states, for both BH_2 and B, to a *diabatic* representation. This will be discussed in the next section. We shall use the calculated matrix elements of the electronic angular momentum operator L to determine an approximate diabatic representation, as advocated some years ago by Rebentrost and Lester.[12]

III. DETERMINATION OF APPROXIMATE DIABATIC POTENTIALS FROM ADIABATIC ENERGIES

Asymptotically, without loss of generality one can choose the three degenerate states of the B atom to correspond to a nominal orientation of the B 2*p* orbital along **R** (P_z), perpendicular to **R** but still in the triatomic plane (P_x), and, finally, perpendicular both to **R** and to the triatomic plane (P_y). As the B atom approaches the H_2 molecule, the lowest two adiabatic states of A' symmetry can, to a good approximation, be thought of as representing a 2×2 orthogonal transformation of the two, asymptotically degenerate, diabatic states of A' symmetry (P_x and P_z). This transformation can be represented by a single transformation angle $\gamma(R,\theta)$, as follows:

$$\begin{bmatrix} 1A' \\ 2A' \end{bmatrix} = \begin{bmatrix} \cos\gamma & \sin\gamma \\ -\sin\gamma & \cos\gamma \end{bmatrix} \begin{bmatrix} P_x \\ P_z \end{bmatrix}. \tag{5}$$

A physically more meaningful, but equivalent interpretation, identifies the angle γ as representing an orthogonal *rotation* of the pair of in-plane orbitals p_x and p_z. The magnitude of this rotation depends on the position of the H_2 molecule. For perpendicular, C_{2v}, geometry the A_1 state always lies above the B_1 state (see Fig. 3), so that the rotation angle in Eq. (5) is always 0°. For linear geometry the angle γ is 90° at long range, where the Σ state (p_z) lies below the Π state (p_x), but switches to 0° at shorter range, where the Π state crosses below the Σ state.

For the van der Waals interaction of an atom with a single *p* electron outside a closed shell and a closed shell molecule, where the interaction is expected to be weak and no bonds are formed, it is physically reasonable to anticipate that the electronic orbital angular momentum **L** of the B atom will be little quenched by the presence of the H_2 molecule, except, perhaps, high on the repulsive wall of the potential. This is the so-called "pure precession" approximation common in diatomic molecular spectroscopy,[39,40] and is equivalent to our approximation that the wave functions for the two states of A' symmetry can be considered

to represent only an orthogonal rotation of two configuration state functions corresponding to $B(2p_z)H_2$ and $B(2p_x)H_2$.

Consider the geometry of Fig. 1(b), where the B atom is fixed on the z axis and the H_2 molecule is rotated in the xz plane. The matrix representation of the operator L_x in a basis of three Cartesian p orbitals (p_x, p_y, and p_z) fixed on the B atom is

$$\begin{array}{c} \\ x \\ y \\ x \end{array}\begin{array}{c} \begin{array}{ccc} x & y & z \end{array} \\ \begin{bmatrix} 0 & 0 & 0 \\ 0 & 0 & -i \\ 0 & i & 0 \end{bmatrix} \end{array}. \tag{6}$$

If, however, the nominally P_x and nominally P_z states are rotated to form the $1A'$ and $2A'$ adiabatic states, as described by Eq. (5), then the calculated matrix of the L_x operator in the basis of the $1A'$, $2A'$, and $1A''$ electronic states would be

$$\begin{array}{c} \\ 1A' \\ 1A'' \\ 2A' \end{array}\begin{array}{c} \begin{array}{ccc} 1A' & 1A'' & 2A' \end{array} \\ \begin{bmatrix} 0 & i\sin\gamma & 0 \\ -i\sin\gamma & 0 & -i\cos\gamma \\ 0 & i\cos\gamma & 0 \end{bmatrix} \end{array}. \tag{7}$$

Similarly, the matrix of the L_z operator is

$$\begin{array}{c} \\ 1A' \\ 1A'' \\ 2A' \end{array}\begin{array}{c} \begin{array}{ccc} 1A' & 1A'' & 2A' \end{array} \\ \begin{bmatrix} 0 & -i\cos\gamma & 0 \\ i\cos\gamma & 0 & -i\sin\gamma \\ 0 & i\sin\gamma & 0 \end{bmatrix} \end{array}. \tag{8}$$

Consequently, after an *ab initio* determination of the matrix elements of L_x (or L_z), one could use either of these two matrices to determine the diabatic→adiabatic transformation angle as, for example,

$$\gamma = \tan^{-1}\langle 1A'|L_x|1A''\rangle / \langle 2A'|L_x|1A''\rangle. \tag{9}$$

Figure 4 represents the dependence of this rotation angle γ as a function of the B–H_2 distance for several values of the B–H_2 angle, calculated using Eq. (9) and the off-diagonal MR-CI matrix elements of L_x. In a simplistic treatment one could consider two limiting models, as illustrated in Fig. 5. In the first, the lowest energy state of A' symmetry would correspond to the B $2p$ orbital being aligned parallel to the H_2 bond axis, regardless of the orientation of the B atom with respect to this axis. In this model, the rotation angle of Eq. (5) would be $\pi-\theta$. In the second limiting model, the lowest energy state of A' symmetry would correspond to the B $2p$ orbital being aligned perpendicular to the B–H_2 axis, regardless of the orientation of the B atom. In this model the rotation angle of Eq. (5) would be 0. We see clearly from Fig. 4 that the first model appears to be a reasonably good description at long range, whereas the second appears to be valid at short range, where the lower energy state of A' symmetry always corresponds to the B $2p$ orbital oriented *perpendicular* to the B–H_2 axis.

The preceding several paragraphs have presented a simple method for the determination of the 2×2 transformation angle in Eq. (5), which is based on the physically reasonable, albeit simplistic, description of the B···H_2 van der Waals molecule. More accurately, this angle could be determined from the fundamental derivative relationship,

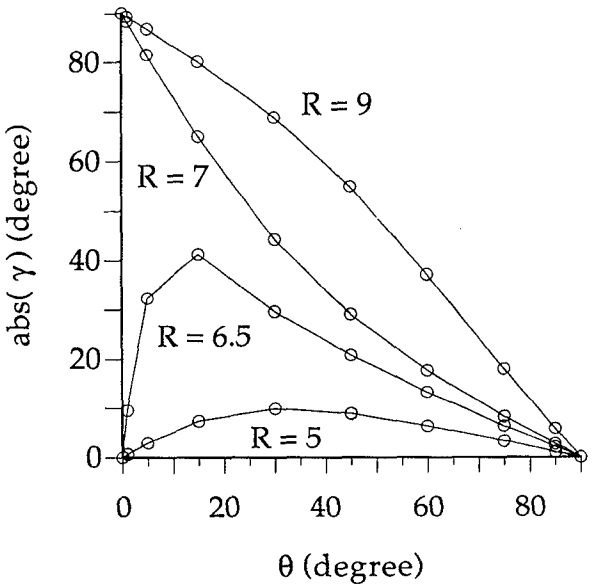

FIG. 4. Values of the diabatic→adiabatic transformation angle γ as a function of the Jacobi BH_2 angle at values of the center-of-mass separation of R=5, 6.5, 7, and 9 bohr.

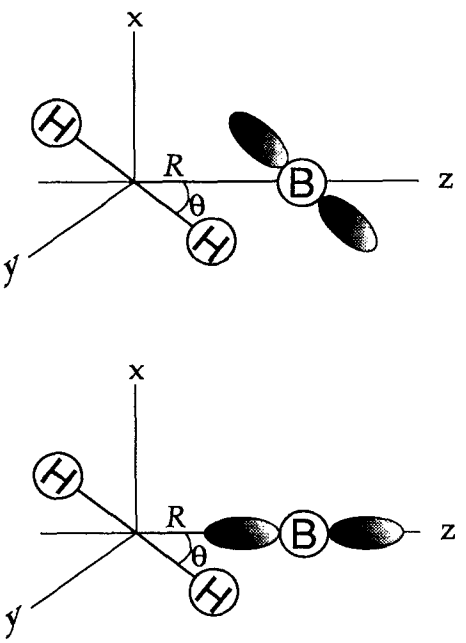

FIG. 5. Simplistic models for the orientation of the B $2p$ orbital corresponding to the lower energy B···H_2 state of A' symmetry. In the model depicted in the upper panel the lower energy corresponds to the $2p$ orbital aligned along the H_2 bond, regardless of the orientation of the B atom. In this case the rotation angle of Eq. (4) is $\pi-\theta$. In the model depicted in the lower panel, the lower energy corresponds to the $2p$ orbital aligned along the vector **R** which connects the B atom to the center-of-mass of the H_2 molecule.

$$\partial\gamma(R,\theta)/\partial q = \langle 1A'|\partial/\partial q|2A'\rangle, \quad (10)$$

where q designates any nuclear coordinate. These derivative coupling matrix elements can be evaluated either analytically[40,41] or by finite difference techniques.[11,12,41,42] The transformation angle itself could then be determined by integration of Eq. (10) and the knowledge that $\gamma(R,\theta)$ vanishes for collinear geometry ($\theta=0$). As discussed recently by Yarkony,[43] our approach to the construction of the diabatic representation, which utilizes matrix elements of the electronic orbital angular momentum **L**, does not, in general, provide the fundamental information on the derivatives with respect to the *internal* (body-frame) coordinates required by Eq. (10). However, in the case of the $F(2s2p^5\ ^2P)+H_2$ system, Rebentrost and Lester[12] found good agreement between the approximate adiabatic→diabatic transformation angle determined by Eq. (9) and the more exact values determined by numerical differentiation of the adiabatic wave functions.

With a knowledge of the transformation angle γ, the energies in the diabatic (P_x,P_y,P_z) basis can be obtained as follows:

$$E_{xx} \equiv \langle P_x|V|P_x\rangle = \cos^2\gamma E_{1A'} + \sin^2\gamma E_{2A'}, \quad (11a)$$

$$E_{zz} \equiv \langle P_z|V|P_z\rangle = \sin^2\gamma E_{1A'} + \cos^2\gamma E_{2A'}, \quad (11b)$$

$$E_{xz} \equiv \langle P_z|V|P_x\rangle = \sin\gamma\cos\gamma(E_{1A'} - E_{2A'}). \quad (11c)$$

An identical transformation can be carried out for the two states of A' symmetry which arise in the counterpoise calculations of the energy of the B atom in the full BH_2 orbital space. Here too, the approximate diabatic states again correspond to an orientation of the in-plane $2p$ orbital, respectively, along **R** and perpendicular to **R**. We will designate these diabatic energies as E^B_{xx}, E^B_{zz}, and E^B_{xz}.

Analogous to Eq. (2) it is now possible to define interaction potentials, for a fixed B–H_2 Jacobi angle γ, as

$$V_{xx}(R) = E_{xx}(R) - E_{H_2}(R) - E^B_{xx}(R), \quad (12a)$$

$$V_{zz}(R) = E_{zz}(R) - E_{H_2}(R) - E^B_{zz}(R), \quad (12b)$$

and

$$V_{xz}(R) = E_{xz}(R) - E_{H_2}(R) - E^B_{xz}(R). \quad (12c)$$

Finally, there exists a *fourth* interaction potential, which corresponds to the single state of A'' symmetry. This state, and consequently its energy, is unaffected by the adiabatic→diabatic transformation. We thus define

$$V_{yy}(R) = E_{A''}(R) - E_{H_2}(R) - E^B_{A''}(R). \quad (13)$$

In the diabatic representation the *three* adiabatic potential energy surfaces ($V_{1A'}$, $V_{2A'}$, and $V_{1A''}$) become replaced by *four* potential energy functions; three diagonal terms (V_{xx}, V_{zz}, and V_{yy}) and one off-diagonal term (V_{xz}). Obviously, the V_{xx} and V_{yy} interaction potentials are identical for collinear geometry, where they correspond to the energies of the two degenerate components of a Π electronic state. Additionally, in collinear, as well as perpendicular (C_{2v}) geometry, the transformation angle is either 0° or 90°, so that there is no mixing of the P_x and P_z states, only a possible energy reordering. Thus the off-diagonal potential energy function V_{xz} vanishes for collinear and perpendicular geometries.

For interactions involving a *homonuclear* diatomic molecule, each of the three adiabatic potential energy surface (PES) must satisfy the symmetry relation $V(R,\pi-\theta) = V(R,\theta)$. A similar symmetry relation will also apply to the three diagonal diabatic potentials, V_{xx}, V_{yy}, and V_{zz}. In our simple picture the off-diagonal term V_{xz} represents the coupling, induced by approach of the H_2 molecule, between two B $2p$ orbitals, one oriented parallel to R and the other perpendicular to R. Because of the directionality of the orbital oriented perpendicular to R (for $0°<\theta<\pi/2$ the *negative* lobe of the $2p$ orbital will lie nearer the center-of-charge of the H_2 while for $\pi/2<\theta<\pi$ the *positive* lobe of the $2p$ orbital will lie nearer), the V_{xz} term will *change sign* as θ goes to $\pi-\theta$. This will guarantee the vanishing of V_{xz} in perpendicular geometry, as desired.

In Fig. 6 we display contour plots of the three *adiabatic* interaction potentials. We remind the reader again that the counterpoise corrections to these adiabatic energies, which are included in these contour plots, can be incorporated meaningfully only after transformation to the approximate diabatic basis, as outlined in Eq. (11). The $1A'$ potential energy surface is lowest in energy, with the minimum in perpendicular geometry ($^2B_2$ symmetry) at a B–H_2 distance of 3.11 Å, and a dissociation energy D_e of 121 cm^{-1}. The $1A''$ potential energy surface, corresponding to the out-of-plane orientation of the B $2p$ orbital, also has a minimum in perpendicular geometry ($^2B_1$ symmetry) at a B–H_2 distance of 3.35 Å, and a dissociation energy D_e of 68 cm^{-1}. The higher potential energy surface of A' symmetry ($2A'$) is repulsive in perpendicular geometry, but has an attractive well in collinear geometry (Σ symmetry) at a B–H_2 distance of 3.93 Å, and a dissociation energy D_e of 75 cm^{-1}.

For subsequent treatments of the dynamics of the B···H_2 system, it will be useful to develop a global representation of the diabatic potentials, fitted from the discrete set of energies obtained from the calculated *ab initio* adiabatic energies. The subtleties underlying the choice of a suitable representation for the angular dependence of the potential will be discussed in the next section.

IV. EXPANSION OF THE POTENTIAL ENERGY FUNCTIONS

To develop an appropriate formal expansion for the diabatic potential energy functions which describe the interaction between an atom in a P electronic state and a closed-shell diatomic molecule, Rebentrost and Lester[12] were guided by the asymptotic form of the quadrupole–quadrupole interaction. Here we present a more rigorous justification, but which leads to the same functional form. We follow closely our earlier description[44] of the interaction between a closed-shell atom and a diatomic molecule in a Π electronic state. Only those details which differen-

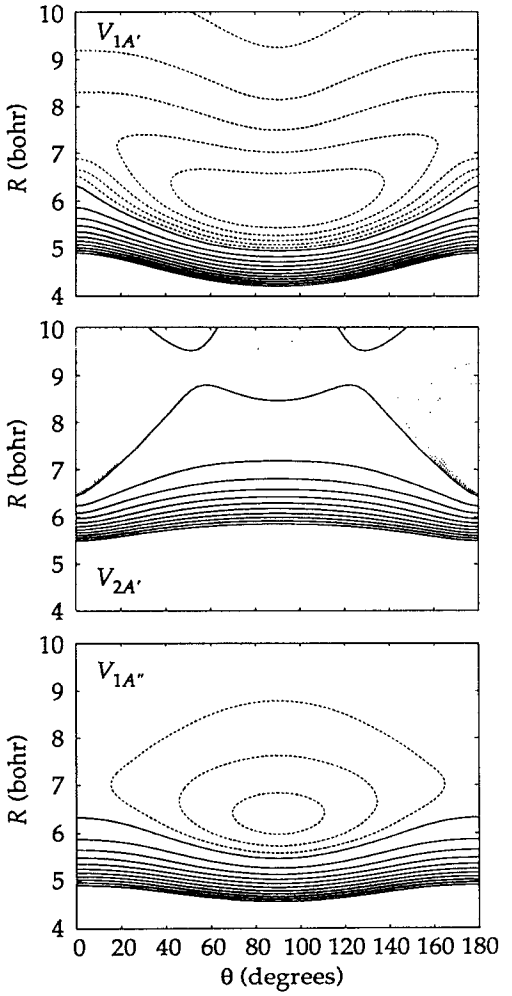

FIG. 6. Contour plots of the lowest three B···H_2 *adiabatic* PES's as determined by MR-CI(D) calculations. The solid contours indicate *positive* interaction energies ranging upwards from 0 in steps of 50 cm^{-1}. The dashed contours (in the contour plots of the $1A'$ and $1A''$ PES's) indicate *negative* interaction energies ranging down from -20 cm^{-1} in steps of 20 cm^{-1}. The dotted contours (in the contour plot of the $2A'$ PES) indicate *negative* interaction energies ranging down from -2 cm^{-1} in steps of 2 cm^{-1}.

tiate the present application from this previous case will be explicitly emphasized here; we refer the interested reader to this earlier paper for more detail.

Designating the electronic wave functions of the isolated atom and molecule as ψ_a and ψ_m, respectively, we can write the matrix elements of the electrostatic interaction potential as

$$V_{a'a}=\left\langle \psi_m\psi_{a'}\left|\sum_{ij} r_{m_i a_j}^{-1}\right|\psi_m\psi_a\right\rangle, \tag{14}$$

where we use atomic units so that $e^2=1$; $r_{ma}=|\mathbf{r}_m-\mathbf{r}_a|$ is the distance between any two charged particles in the molecule and the atom; and the sum runs over all the charged particles in the atom and molecule. Here we have assumed that electronic excitation of the molecule does not occur.

The inverse distance can be expanded in the usual multipolar series[45]

$$r_{m_i a_j}^{-1}=\sum_{\substack{ll_1l_2\\ mm_1m_2}} (lml_1m_1|l_2m_2)A_{ll_1l_2}(r_{m_i},r_{a_j},R)\times C_{lm}(\hat{r}_{m_i})C_{l_1m_1}(\hat{r}_{a_j})C^*_{l_2m_2}(\hat{R}), \tag{15}$$

where $(\cdots\cdots|\cdots)$ is a Clebsch–Gordan coefficient[46] and $C_{lm}(\hat{R})$ is an unnormalized spherical harmonic[46] Further, $\hat{r}_{m_i}$ and $\hat{r}_{a_j}$ designate two, identically oriented coordinate systems, one fixed in the molecule and the other in the atom. If a "body-fixed" orientation of these coordinate systems is chosen, in which the z axes lie along $\hat{R}$, then only terms with $m_2=0$ will contribute, since $C_{l_2m_2}(\hat{z})=\delta_{m_20}$.

The molecular electronic wave function is, however, defined in the *molecular* frame where the z axis is the bond axis. Let Ω_{MB} be the rotation, with Euler angles $0\theta0$, which describes the rotation of the body frame onto the molecular frame. This choice of Euler angles implies that the y axes coincide in both frames, and, furthermore, that the xz planes coincide with $\theta=\pi/2$. The first spherical harmonic in Eq. (15) transforms as[46]

$$C_{lm}(\hat{r}_{m_i})=\sum_{\mu} D^{l*}_{m\mu}(0\theta0)C_{l\mu}(\hat{\rho}_i), \tag{16}$$

where $\hat{\rho}_i$ describes the orientation of the ith electron in the molecular frame and $D^{l*}_{m\mu}$ is a rotation matrix element.[46] For interactions involving a molecule in a Σ electronic state (as, for example, H_2), only the $\mu=0$ terms will survive the integration over the molecular coordinates implicit in Eq. (14).

We now designate the atomic wave functions by $\psi_a=|\Lambda\rangle$, where in these "signed-Λ" states the quantum number $\Lambda(\Lambda=0,\pm1)$ denotes the body-frame projection of the electronic orbital angular momentum. Introducing Eq. (16) into Eq. (15), and then carrying out the integrations over the electronic coordinates implicit in Eq. (14), we obtain the following expression for the electrostatic potential:

$$V_{\Lambda',\Lambda}(R,\theta)\equiv V_k(R,\theta)=\sum_l V_l^k(R)\,D^{l*}_{\Lambda-\Lambda',0}(0\theta0), \tag{17}$$

where k is an index (to be discussed below) which contains information on the values of Λ and Λ'. In this equation

$$V_l^k(R)=\langle\Lambda'|\langle\psi_m|\sum_{ijl_1l_2m}(lml_1-m|l_20)A_{ll_1l_2}(r_{m_i},r_{a_j},R)\times C_{l0}(\hat{\rho}_i)C_{l_1-m}(\hat{r}_{a_j})|\psi_m\rangle|\Lambda\rangle. \tag{18}$$

The azimuthal symmetry of the atomic wave function about R implies that the atomic wave functions can be expressed, at least formally, as

$$|\Lambda\rangle=\sum_L U_L(r_a)C_{L\Lambda}(\hat{r}_a). \tag{19}$$

TABLE I. The expansion of the interaction potential $V_{\Lambda',\Lambda}(R,\theta)$ for the approach of an atom in a P electronic state to a cylindrical, closed-shell molecule. Here $\Lambda=0, \pm 1$ designates the projection of the electronic orbital angular momentum along the vector **R** which joins the atom to the center-of-mass of the molecule.[a]

	Λ		
Λ'	1	0	−1
1	$\sum_{l=0} V_l^{\pi\pi}(R)\ d^l_{00}(\theta)$	$-2^{1/2}\sum_{l=1} V_l^{\pi\sigma}(R)\ d^l_{10}(\theta)$	$\sum_{l=2} V_l^{\delta}(R)\ d^l_{20}(\theta)$
0	$2^{1/2}\sum_{l=1} V_l^{\pi\sigma}(R) d^l_{10}(\theta)$	$\sum_{l=0} V_l^{\sigma}(R)\ d^l_{00}(\theta)$	$-2^{1/2}\sum_{l=1} V_l^{\pi\sigma}(R)\ d^l_{10}(\theta)$
−1	$\sum_{l=2} V_l^{\delta}(R)\ d^l_{20}(\theta)$	$2^{1/2}\sum_{l=1} V_l^{\pi\sigma}(R)\ d^l_{10}(\theta)$	$\sum_{l=0} V_l^{\sigma}(R)\ d^l_{00}(\theta)$

[a]See Eq. (17) of text. Although the summation in the terms involving the $V_{\pi\sigma}$ potential energy functions extends from $l=1$, for interactions involving a *homonuclear* molecule all odd-l terms will vanish, as discussed in the text.

The integration over $\hat{r}_{a_j}$ in Eq. (18) will thus involve integrals of the type

$$\sum_{LL'm}\int C^*_{L'\Lambda'}(\hat{r}_{a_j})C_{l_1-m}(\hat{r}_{a_j})C_{L\Lambda}(\hat{r}_{a_j})d\hat{r}_{a_j}, \tag{20}$$

which can be integrated to give[46]

$$4\pi\delta_{m,\Lambda-\Lambda'}(-1)^{\Lambda'}\sum_{LL'}\begin{pmatrix} L' & l_1 & L \\ 0 & 0 & 0\end{pmatrix}\begin{pmatrix} L' & l_1 & L \\ -\Lambda' & -m & \Lambda\end{pmatrix}. \tag{21}$$

It is the Kroenecker delta here, imposed by the denominator of the second $3j$ symbol, which constrains the allowed value of m in the summation in Eq. (18), and determines the projection indices on the rotation matrix element in Eq. (17).

Since only the second Euler angle (θ) is nonvanishing in the Ω_{MB} transformation, the rotation matrix elements in Eq. (17) can be replaced by the *reduced* rotation matrix elements $d^l_{\Lambda-\Lambda'0}(\theta)$. The individual $V_l^k(R)$ terms in Eq. (17) represent the expansion coefficients of the diabatic potential energy function which couples the atomic states $|\Lambda\rangle$ and $|\Lambda'\rangle$ due to approach of the molecule. The symmetry of the $3j$ symbols[46] in Eq. (21) and the relation

$$d^{\ l}_{-m,0}(\theta)=(-1)^m d^{\ l}_{m0}(\theta) \tag{22}$$

imply that the nine individual coupling terms between all three of the $\Lambda=0, \pm 1$ electronic states can be described fully in terms of just *four* distinct potential energy functions (PEF). These we shall designate as $V_{xx}(R,\theta)$, $V_s(R,\theta)$, $V_{xz}(R,\theta)$, and $V_d(R,\theta)$. Here the V_{xx} and the V_{xz} PEF's are identical to those defined in the preceding section. The V_s and V_d PEF's are one-half the sum and one-half the difference of the V_{xx} and V_{yy} PEF's, defined in the preceding section, so that

$$V_{xx}=(V_s-V_d) \tag{23a}$$

and

$$V_{yy}=(V_s+V_d). \tag{23b}$$

Table I summarizes the relation between the $V_{\Lambda',\Lambda}(R,\theta)$ matrix elements and the four diabatic potential energy functions introduced above, $V_{xx}(R,\theta)$, $V_s(R,\theta)$, $V_{xz}(R,\theta)$,

TABLE II. The expansion of the interaction potential for the approach of an atom in a P electron state to a cylindrical, closed-shell molecule, in terms of the real (P_x, P_y, and P_z) Cartesian wave functions. A body frame is used in which the z axis points along the vector **R** which joins the atom to the center-of-mass of the molecule, the x axis lies in the plane of the atom–molecule system, and the y-axis lies perpendicular to this plane (see Fig. 1).[a]

	P_z	P_x	P_y
P_z	$\sum_{l=0} V_l^{\pi\pi}(R)\ d^l_{00}(\theta)$	$\sum_{l=1} V_l^{\pi\sigma}(R)\ d^l_{10}(\theta)$	0
P_x	$\sum_{l=1} V_l^{\pi\sigma}(R)\ d^l_{10}(\theta)$	$\sum_{l=0} V_l^{\sigma}(R)\ d^l_{00}(\theta)-\sum_{l=2} V_l^{\delta}(R)\ d^l_{20}(\theta)$	0
P_y	0	0	$\sum_{l=0} V_l^{\sigma}(R)\ d^l_{00}(\theta)+\sum_{l=2} V_l^{\delta}(R)\ d^l_{20}(\theta)$

[a]Although the summation in the terms involving the $V_{\pi\sigma}$ potential energy functions extends from $l=1$, for interactions involving a *homonuclear* molecule all odd-l terms will vanish, as discussed in the text.

and $V_d(R,\theta)$. Table I also specifies the identification of the index k in Eq. (17). Each of the four diabatic potential energy functions can subsequently be expanded in terms of reduced rotation matrix elements. This, too, is summarized in Table I.

It is straightforward to make the connection between the $V_{\Lambda',\Lambda}(R,\theta)$ PEF's and the diabatic atom–molecule potential energy surfaces, which were introduced in the preceding section in terms of the real (Cartesian) atomic wave functions, P_x, P_y, and P_z. We know $|P_z\rangle = |\Lambda=0\rangle$ and[46]

$$|P_{x,y}\rangle = 2^{-1/2}(-|\Lambda=1\rangle \pm |\Lambda=-1\rangle), \tag{24}$$

where the plus and minus signs are associated with, respectively, the P_x and P_y states. Table II summarizes the expansion of the interaction potential in the basis of the P_x, P_y, and P_z wave functions.

Obviously, there is no coupling between the two wave functions (P_x and P_y) which are *symmetric* (A') and the sole function (P_y) which is *antisymmetric* (A'') with respect to reflection of the electronic coordinates in the triatomic plane. Further, since $\lim_{\theta\to 0,\pi} d^l_{m0}(\theta) = 0$ whenever $m>0$, it is clear from Table II, as anticipated already in the preceding section, that the B···H_2 V_{xx} and V_{yy} interaction potentials are identical for collinear geometry, where they correspond to the energies of the two degenerate components of a Π electronic state.

As discussed in the preceding section, the V_{xx}, V_{yy}, and V_{zz} PEF's must satisfy the symmetry relation $V(R,\pi-\theta)=V(R,\theta)$. This implies that the odd-l coefficients in the expansions of the $V_{xx}(R,\theta)$, $V_s(R,\theta)$, and $V_d(R,\theta)$ PEF's will vanish, because[46]

$$d^{\,l}_{m0}(\pi-\theta) = (-1)^{l+m} d^{\,l}_{m0}(\theta). \tag{25}$$

Furthermore, as discussed in the preceding section, the V_{xz} PEF must vanish for perpendicular geometry ($\theta=\pi/2$). Thus, Eq. (24) implies that the odd-l coefficients in the expansion of the $V_{xz}(R,\theta)$ PEF similarly vanish. This fact was also noted by Rebentrost and Lester.[12]

The informed reader might recognize a close similarity between the description of interaction between an *atom* in a ^2P electronic state with a closed-shell *molecule* and the interaction between a *molecule* with closely spaced $^2\Pi$ and $^2\Sigma$ electronic states and a closed-shell atom. Examples of the latter, studied earlier, are CN($X\,^2\Sigma^+$,$A\,^2\Pi$)–He (Refs. 47–51) and N_2^+ ($X\,^2\Sigma_g^+$,$A\,^2\Pi_u$).[50,52]

At long range, the V_{zz}, V_s, and V_d B···H_2 PEF's will be dominated by the interaction between the quadrupole moment of the H_2 molecule and that of the B atom.[53] With the known[53] expression for the geometry dependence of the quadrupole–quadrupole interaction, we have

$$\lim_{R\to\infty} V(R,\theta) = \tfrac{3}{4} Q_{H_2} Q_B f(\theta) R^{-5}. \tag{26}$$

Here $f(\theta)=12\cos^2\theta-4$ for the V_{zz} PEF, $2-6\cos^2\theta$ for the V_s PEF, and $\cos^2\theta-1$ for the V_d PEF. Multireference configuration interaction calculations with the same (avtz) basis set used in the full B···H_2 calculations yielded the following values of the quadrupole moments: Q_{H_2} = 0.4615 a.u. and $Q_B=-2.3439$ a.u.

With this in mind, for each fixed value of θ_i used in the *ab initio* calculations (1°, 5°, 15°, 30°, 45°, 60°, 75°, 85°, and 90°) we fit the resulting $V_{zz}(R,\theta)$, $V_s(R,\theta)$, $V_{xz}(R,\theta)$, and $V_d(R,\theta)$ PEF's, as a function of R, as follows: for $V_{zz}(R,\theta)$, $V_s(R,\theta)$, and $V_d(R,\theta)$,

$$\begin{aligned} V(R,\theta_i) = {} & c_1\exp(-b_1R)+(c_2+c_3R)\exp(-b_2R) \\ & -c_4S(R,R_0)/R^6 \\ & +\tfrac{3}{4}Q_{H_2}Q_B f(\theta_i)S(R,7)/R^5, \end{aligned} \tag{27}$$

where

$$S(R,R_0) = \tfrac{1}{2}\{\tanh[1.2(R-R_0)]-1\}. \tag{28}$$

Finally, the V_{xz} PEF, to which there is no quadrupole–quadrupole contribution, was fitted as follows:

$$V_{xz}(R,\theta_i) = \exp(c_1+c_2/R+c_3/R^2+c_4/R^3). \tag{29}$$

Of course, in Eqs. (27) and (29), the expansion parameters (R_0, b_j, and c_j) depend on the particular value of θ_i chosen.

Subsequently, at any value of R, the expansion coefficients in terms of the reduced rotation matrix elements [the $V_l^k(R)$ of Eq. (17)] are obtained by a least squares fit. We found that an excellent representation could be achieved by limiting the expansion to the four lowest possible values of l(l=0, 2, 4, and 6).[54]

Figure 7 displays contour plots of the variation with the B···H_2 angle of the V_{xx}, V_{zz}, and V_{xz} approximate *diabatic* PEF's.

V. PREDICTED STRUCTURE OF THE B···*p*-H_2 VAN DER WAALS MOLECULE

In principle, with the approximate diabatic potential energy functions determined above, one could determine the wave function, and concomitantly, the energy levels for the B($2s2p\,^2P$)···H_2 van der Waals molecule. To do so one could use basis functions formed by coupling the atomic electronic angular momenta **L** and **S** to form **J**, the total angular momentum of the atom, and then **J** with **j**, the angular momentum of the hydrogen atom, to form $\mathbf{j}_{12}$. This latter would be coupled with **l**, the orbital angular momentum of the B···H_2 pair to form the total angular momentum $\mathbf{J}_t$. The resulting expressions for the matrix elements of the electrostatic potential in this Hund's case (e) basis[55–58] are exceedingly complicated.

A simplification occurs if one constrains molecular hydrogen to its lowest ($j=0$) rotational level, without possibility of excitation to or mixing with the higher (j=2, 4,...) rotational states of *p*-H_2. In this case the H_2 can be considered a spherical atom, and the B($2s2p\,^2P$)···H_2 system becomes equivalent to the interaction of an atom in a ^2P electronic state with a spherical, closed-shell partner.[56,59] The V_Σ and V_Π potentials which describe the interaction between the atom and spherical partner when the p orbital is pointed, respectively, along and perpendicular to the internuclear axis, are given by the spherically sym-

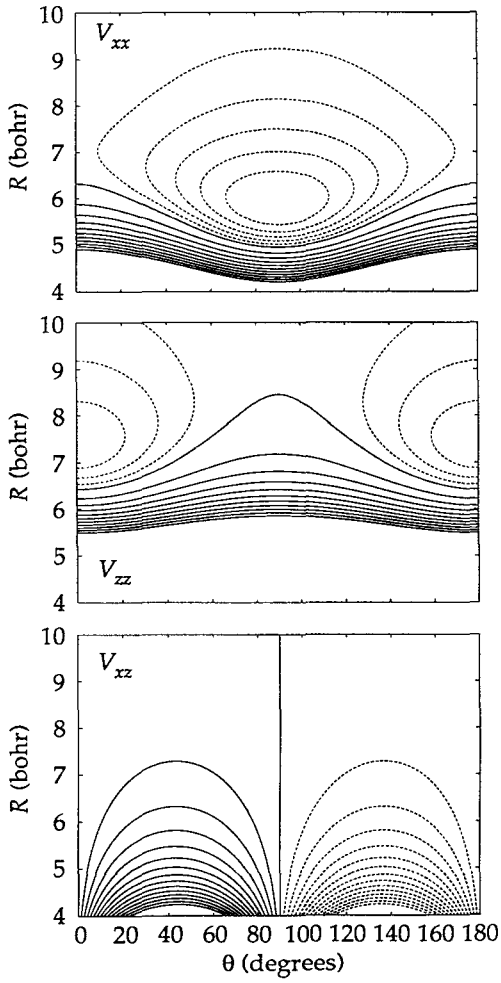

FIG. 7. Contour plots of the V_{xx}, V_{zz}, and V_{xz} B···H_2 approximate *diabatic* PES's as determined by MR-CI(D) calculations and the adiabatic→diabatic transformation described in Sec. III. The V_{xx} and V_{zz} PES's correspond to the interaction energy for approach of the B atom with the $2p$ orbital pointing, respectively, along **R** and perpendicular to **R** but in the BH_2 plane. The V_{xz} PEF represents the off-diagonal electrostatic coupling between these two states of A' symmetry. The solid contours indicate *positive* interaction energies ranging upwards from 0 in steps of 50 cm^{-1}. The dashed contours indicate *negative* interaction energies. In the case of the V_{xx} and V_{zz} PEF's these range down from -20 cm^{-1} in steps of 20 cm^{-1}, and, in the case of the V_{xz} PEF, down from -50 cm^{-1} in steps of 50 cm^{-1}.

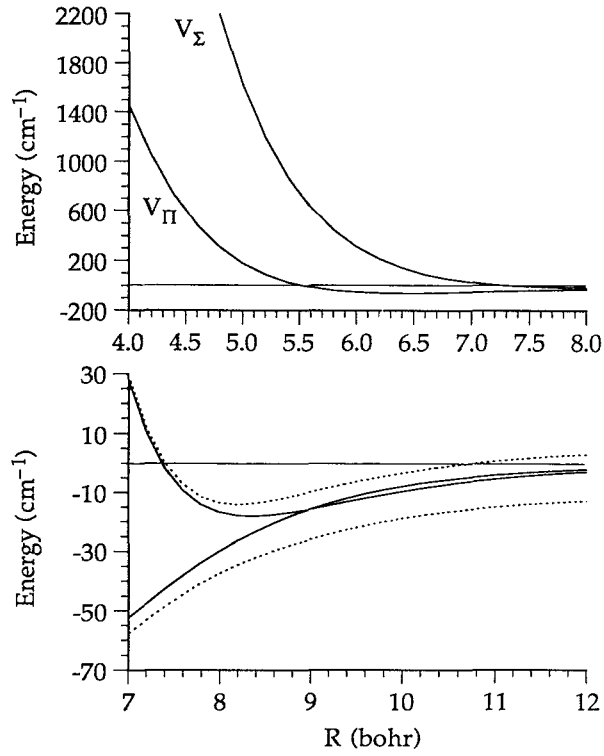

FIG. 8. (Upper) Interaction potentials [$V_\Pi(R)$ and $V_\Sigma(R)$] for the states of Π and Σ^+ symmetry which characterize the interaction of a spherical H_2 molecule ($j=0$) with a B ^2P atom. These potentials are identical to the spherically symmetric ($l=0$) components in the expansions of, respectively, the V_s and V_{zz} diabatic PEF's. (Lower) The solid curves represent the $V_\Pi(R)$ and $V_\Sigma(R)$ curves in the long-range region. The dashed curves are the fully adiabatic energies arising from diagonalization of the 2×2 Hamiltonian of Eq. (30).

metric ($l=0$) terms in the expansion of the $V_{zz}(V_\Sigma)$ and $V_s(V_\Pi)$ PEF's defined and discussed above. These two potential curves are displayed in Fig. 8.

For the lowest rotational level of the van der Waals complex ($J_t=1/2$), there will exist only two levels of *e*-parity ($J=1/2$, $l=1$ and $J=3/2$, $l=1$) and two levels of *f*-parity ($J=1/2$, $l=0$ and $J=3/2$, $l=2$). In both cases the matrix of the Hamiltonian (in the so-called "pure-precession" approximation[39,40] that neither the atomic spin–orbit constant nor the electronic orbital motion of the p electron are effected by the partner) in this 2×2 basis is given by[59]

$$\begin{array}{c} \\ J=1/2 \\ J=3/2 \end{array}\begin{array}{c} \begin{array}{cc} J=1/2 & J=3/2 \end{array} \\ \begin{bmatrix} V_0+Bl(l+1)-a & 2^{1/2}V_2 \\ 2^{1/2}V_2 & V_0+V_2+Bl(l+1)+\frac{1}{2}a \end{bmatrix} \end{array}. \tag{30}$$

Here,

$$V_0=[2V_\Pi(R)+V_\Sigma(R)]/3$$
$$=[2V^S_{l=0}(R)+V^{zz}_{l=0}(R)]/3, \tag{31}$$

and[60]

$$V_2=[-V_\Pi(R)+V_\Sigma(R)]/3, \tag{32}$$

while $B=\hbar^2/2\mu R^2$, where μ is the B–H_2 reduced mass, and a is the B atom spin–orbit constant ($a=10.7$ cm^{-1}).[61]

The off-diagonal coupling term, $2^{1/2}V_2(R)$, is proportional to the difference between the $V_\Pi(R)$ and $V_\Sigma(R)$ potential curves. For distances inside of $R\cong7.5$ bohr, this difference rapidly becomes much larger than the small spin–orbit splitting. At that point, and if the small difference between the centrifugal barriers to the two states is ignored, the 2×2 matrix of Eq. (30) can be diagonalized to yield two states, one with energy $V_\Pi(R)$ and the other with energy $V_\Sigma(R)$. Physically, as the splitting between the Σ and Π curves becomes large, the orientation of the B atom p orbital becomes uncoupled from the spin and cou-

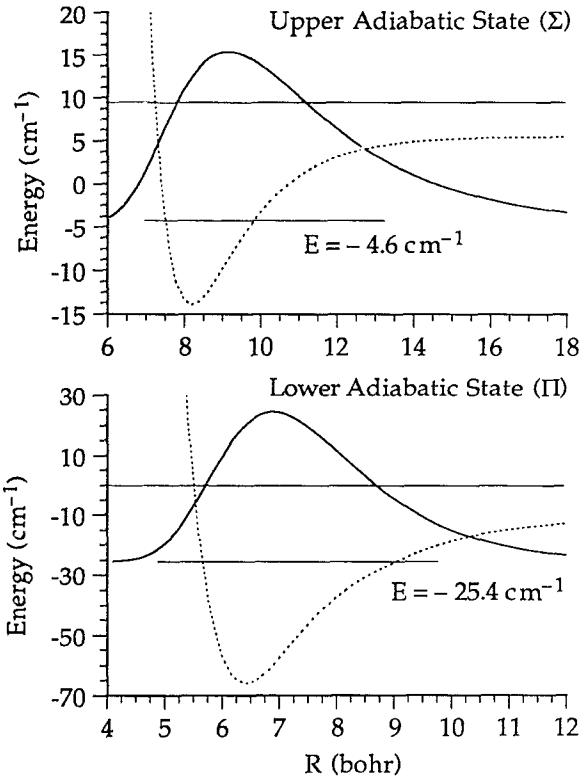

FIG. 9. (Upper) Plot of the $^{11}B(^2P)H_2(j=0)$ vibrational wave function for the sole bound vibrational state of the *upper* fully adiabatic potential displayed as a dashed curve (also in the lower panel of Fig. 8). The zero-point corrected dissociation energy is 4.6 cm^{-1}. (Lower) Identical plot but for the wave function of the *lower* fully adiabatic potential. The zero-point corrected dissociation energy is 25.4 cm^{-1}.

pled to the intermolecular axis, the classic Hund's case (e) → Hund's case (a) recoupling which characterizes the approach of a ^2P atom to a closed-shell spherical partner.[56–58]

To a very good approximation, then, the lowest energy level(s) of a B···p-H_2 van der Waals molecule in the $J_t=1/2$ rotational level can be determined by solution of a one-dimensional Schrödinger equation governed by the lower root of the diagonalization of the 2×2 Hamiltonian given by Eq. (30). In fact, the zero point energy is so large that there exists only *one* bound vibrational level in this potential with a dissociation energy of 25.4 cm^{-1}. The lower panel of Fig. 9 displays the corresponding wave function, which we see is very broad, due to the light reduced mass of the B–H_2 system. The expectation value of the B–H_2 distance is $\langle R\rangle=7.61$ bohr, considerably larger than the location of the minimum in the potential ($R_e=6.41$ bohr, see Fig. 8). A measure of the width of the wave function is given by $\langle(R-\langle R\rangle)^2\rangle^{1/2}=1.07$ bohr. The upper root of the same 2×2 Hamiltonian, which resembles closely the $V_\Sigma(R)$ potential, also supports one bound state, with, however, a much smaller dissociation energy ($D_0=4.6$ cm^{-1}). The wave function, also shown in Fig. 9, is even broader than that for the nominally Π state [$\langle R\rangle=9.96$ bohr, $\langle(R-\langle R\rangle)^2\rangle^{1/2}=1.75$ bohr].

The approximation that the van der Waals complex of p-H_2 with B can be treated under the assumption of a spherical H_2 molecule is consistent with earlier work or the dynamics of small clusters of p-H_2.[62–64] Because of the considerable anisotropy of the lowest B–H_2 potential energy surface (see the upper panel of Fig. 6), some distortion from sphericity might well occur, accompanied by an increase in the zero-point corrected dissociation energy. This will be the object of further investigation.[65]

In the absence of a magnetic catalyst, the interconversion of para and ortho hydrogen is very slow. Thus we would anticipate that the lowest rotational level of o-H_2 ($j=1$) would also form a bound van der Waals complex with B($2s^22p\ ^2P$). If anything, the dissociation energy would be somewhat *higher* than that of B···p-H_2, since a rotating hydrogen molecule in $j=1$ with a body-frame projection of $m_j=\pm1$ can better keep out of the way of the B atom than a rotationless, spherical H_2. However, the determination of the bound state wave function and energy will be considerably more complicated, due to the additional angular momentum coupling which must be introduced into the basis states used to expand the wave function.

VI. CONCLUSION

We have presented here the results of multireference configuration-interaction calculations of the three adiabatic potential energy surfaces which describe the interaction of the B atom in its $2s^22p\ ^2P$ electronic ground state with molecular hydrogen. The minimum energy is predicted to occur in C_{2v} geometry with an electronic symmetry of $^2B_1$, at a B–H_2 distance of 3.11 Å, and a dissociation energy D_e of 121 cm^{-1}. Although higher-order excitations (triple, quadruple, ...) out of the CASSCF reference wave function were taken into account approximately, we believe that the true dissociation energy will be ~20 cm^{-1} larger than the predicted value.

An approach originally introduced by Rebentrost and Lester for the F(^2P)+H_2 system,[12] was used to obtain the transformation to an approximate diabatic representation, in which the three states are characterized by the orientation of the B p orbital with respect to the B–H_2 axis. The transformation was based on calculated *ab initio* values of the matrix elements of the *electronic* orbital angular momentum **L**. The resulting *four* diabatic potential energy functions were then expanded in terms of Legendre and associated Legendre polynomials.

For the interaction of p-H_2 with the B atom, the spherical symmetry of the rotational ground state ($j=0$) reduces the triatomic system to the interaction of a ^2P atom with a closed-shell, spherical target. Since the spin–orbit constant of the B atom is so small, the lowest state of the B···p-H_2 system is governed almost exclusively by the lower (Π-state) B···p-H_2 potential. Because of the high zero-point energy of this light system, there exists only one bound vibrational level, with a dissociation energy of ~25 cm^{-1}. Additionally, a very weakly bound ($D_0\cong5$ cm^{-1}) vibrational state exists for approach of the spherical ($j=0$) H_2 molecule to B governed by the higher energy Σ potential.

The B···p-H_2 potentials calculated here can now serve as the starting point for the study of the structure, energetics, and dynamics of van der Waals clusters of individual B atoms with multiple spherical hydrogens. Concurrently, future work should explore the binding of o-H_2 with B, for an eventual comparison of the relative stabilities of the van der Waals complexes of B with the two nuclear spin isomers of H_2.

In a recent paper[66] Dagdigian and co-workers have reported observations of the B(^2P)···Ar van der Waals molecule. The binding of the Ar atom led to the appearance of molecular satellite bands in the region of the atomic ($2s^23s\ ^2S \leftarrow 2s^22p\ ^2P$) line. A similar experimental technique will be less easily applicable to the B···H_2 molecule, since the addition of $\sim$40 000 cm^{-1} of electronic energy[61] is more than enough for reaction (1) to occur, so that little, if any, fluorescence will be produced subsequent to electronic excitation of B···H_2. We are, nevertheless, hopeful that the experimental detection of B···H_2 will eventually be feasible.

ACKNOWLEDGMENTS

The author wishes to thank the U.S. Air Force Office of Scientific Research for support of the research reported here under Grant No. AFOSR-91-0363. He is also grateful to Hans-Joachim Werner for his invaluable technical advice about the *ab initio* calculations reported here, to David Yarkony for illuminating conversations about the transformation of the adiabatic electronic wave functions, and to Roberta Saxon for discussions of the orbital occupancy of the molecular and van der Waals BH_2 species.

[1] K. P. Huber and G. Herzberg, *Molecular Spectra and Molecular Structure. IV. Constants of Diatomic Molecules* (Van Nostrand Reinhold, New York, 1979).
[2] W. H. Breckenridge, in *Reactions of Electronically Excited Atoms*, edited by A. Fontijn and M. A. A. Clyne (Academic, London, 1983), p. 157.
[3] W. H. Breckenridge and H. Umemoto, Adv. Chem. Phys. **50**, 325 (1982).
[4] W. H. Breckenridge, C. Jouvet, and B. Soep, J. Chem. Phys. **84**, 1443 (1986).
[5] D. Konowalow (to be published).
[6] N. Adams, W. H. Breckenridge, and J. Simons, Chem. Phys. **56**, 327 (1981).
[7] M. Rosenkranz (to be published).
[8] J. A. Boatz, M. Gutowski, and J. Simons, J. Chem. Phys. **96**, 6555 (1992).
[9] X. Yang and P. J. Dagdigian, J. Phys. Chem. **97**, 4270 (1993).
[10] M. E. Fajardo and S. Tam (private communication, 1993).
[11] F. Rebentrost and W. A. Lester, Jr., J. Chem. Phys. **63**, 3737 (1975).
[12] F. Rebentrost and W. A. Lester, Jr., J. Chem. Phys. **64**, 3879 (1976).
[13] F. Rebentrost and W. A. Lester, Jr., J. Chem. Phys. **67**, 3367 (1977).
[14] D. R. Flower and J.-M. Launay, J. Phys. B **10**, L229 (1977).
[15] D. R. Flower and J. M. Launay, J. Phys. B **10**, 3673 (1977).
[16] T. H. Dunning, Jr. and L. B. Harding, in *Theory of Chemical Reaction Dynamics*, edited by M. Baer (Chemical Rubber, Boca Raton, 1985), p. 1.
[17] R. A. Poirier, M. R. Peterson, and M. Menzinger, J. Chem. Phys. **78**, 4592 (1983).
[18] I. Hertel, Adv. Chem. Phys. **50**, 475 (1985).
[19] P. Botschwina, W. Meyer, I. V. Hertel, and W. Reiland, J. Chem. Phys. **75**, 5438 (1981).
[20] H.-J. Werner and W. Meyer, J. Chem. Phys. **74**, 5794 (1981).
[21] P. Halvick and D. G. Truhlar, J. Chem. Phys. **96**, 2895 (1992).
[22] D. W. Schwenke, S. L. Mielke, G. J. Tawa, R. S. Friedman, P. Halvick, and D. G. Truhlar, Research Report No. UMSI 92/271, University of Minnesota Supercomputer Institute, 1993.
[23] D. R. Yarkony, J. Chem. Phys. **84**, 3206 (1986).
[24] G. Herzberg, *Molecular Spectra and Molecular Structure III. Electronic Spectra and Electronic Structure of Polyatomic Molecules* (Van Nostrand, Princeton, 1967).
[25] M. W. Chase, Jr., C. A. Davies, J. R. Downey, Jr., D. J. Frurip, R. A. McDonald, and A. N. Syverud, J. Phys. Chem. Ref. Data **14**, Suppl. 1 (1985).
[26] P.-O. Widmark, P.-A. Malmqvist, and B. O. Roos, Theor. Chim. Acta **77**, 291 (1990).
[27] P. J. Knowles and H.-J. Werner, Chem. Phys. Lett. **115**, 259 (1985).
[28] MOLPRO is a package of *ab initio* programs written by H.-J. Werner and P. J. Knowles, with contributions from J. Almlöf, R. Amos, S. Elbert, W. Meyer, E. A. Reinsch, R. Pitzer, and A. Stone.
[29] W. Meyer, Int. J. Quantum Chem. Symp. **5**, 341 (1971).
[30] W. Meyer, J. Chem. Phys. **58**, 1017 (1973).
[31] W. Meyer, Theor. Chim. Acta **35**, 277 (1974).
[32] T. H. Dunning, Jr., J. Chem. Phys. **90**, 1007 (1989).
[33] R. A. Kendall, T. H. Dunning, Jr., and R. J. Harrison, J. Chem. Phys. **96**, 6796 (1992).
[34] S. F. Boys and F. Benardi, Mol. Phys. **19**, 553 (1970).
[35] R. N. Diffenderfer and D. R. Yarkony, J. Phys. Chem. **86**, 5098 (1982).
[36] B. H. Lengsfield, J. Chem. Phys. **77**, 4073 (1982).
[37] H.-J. Werner and P. J. Knowles, J. Chem. Phys. **89**, 5803 (1988).
[38] E. R. Davidson and D. W. Silver, Chem. Phys. Lett. **53**, 403 (1977).
[39] J. T. Hougen, Natl. Bur. Stand. (U.S.) Monogr. 115 (1970).
[40] H. Lefebvre-Brion and R. W. Field, *Perturbations in the Spectra of Diatomic Molecules* (Academic, New York, 1986).
[41] M. Desouter-Lecomte, J. C. Leclerc, and C. P. J. C. Lorquet, Chem. Phys. **9**, 147 (1975).
[42] G. Hirsch, P. J. Bruna, R. J. Buenker, and S. D. Peyerimhoff, Chem. Phys. **45**, 335 (1980).
[43] D. R. Yarkony, J. Chem. Phys. **90**, 1657 (1989).
[44] M. H. Alexander, Chem. Phys. **92**, 337 (1985).
[45] C. G. Gray, Can. J. Phys. **54**, 505 (1976).
[46] D. M. Brink and G. R. Satchler, *Angular Momentum*, 2nd ed. (Clarendon, Oxford, 1968).
[47] M. H. Alexander and G. C. Corey, J. Chem. Phys. **84**, 100 (1986).
[48] H.-J. Werner, B. Follmeg, and M. H. Alexander, J. Chem. Phys. **89**, 3139 (1988).
[49] H.-J. Werner, B. Follmeg, M. H. Alexander, and D. Lemoine, J. Chem. Phys. **91**, 5425 (1989).
[50] M. H. Alexander, A. Berning, A. Degli-Esposti, A. Jörg, A. Kliesch, and H.-J. Werner, Ber. Bunsenges. Phys. Chem. **94**, 1253 (1990).
[51] P. J. Dagdigian, D. Patel-Misra, A. Berning, H.-J. Werner, and M. H. Alexander, J. Chem. Phys. **98**, 8580 (1993).
[52] A. Berning and H.-J. Werner (to be published).
[53] A. D. Buckingham, Adv. Chem. Phys. **12**, 107 (1967).
[54] A FORTRAN program to compute the four B–H_2 potential energy functions is available by electronic mail (address: mha@hibridon.umd.edu). Please supply a return electronic mail address. A table of the expansion parameters in Eqs. (27)–(29) is also available on request from the author, either by electronic or regular mail.
[55] G. Herzberg, *Spectra of Diatomic Molecules*, 2nd ed. (Van Nostrand, Princeton, 1968).
[56] F. H. Mies, Phys. Rev. A **7**, 942 (1973).
[57] V. Aquilanti and G. Grossi, J. Chem. Phys. **73**, 1165 (1980).
[58] V. Aquilanti, P. Casavecchia, G. Grossi, and A. Laganá, J. Chem. Phys. **73**, 1173 (1980).
[59] R. H. G. Reid, J. Phys. B **6**, 2018 (1973).
[60] For simplicity, our definition of the $V2$ term is one-fifth that of Reid (Ref. 59).
[61] C. E. Moore, *Atomic Energy Levels, NSRDS-NBS 35* (U.S. GPO, Washington, D.C., 1971).
[62] I. F. Silvera and V. V. Goldman, J. Chem. Phys. **69**, 4209 (1978).
[63] M. V. R. Krishna and K. B. Whaley, Z. Phys. D **20**, 223 (1991).
[64] D. Scharf, M. L. Klein, and G. J. Martyna, J. Chem. Phys. **97**, 3590 (1992).
[65] A. Vegiri, M. H. Alexander, S. Gregurick, A. McCoy, and R. B. Gerber (to be published).
[66] E. Hwang, Y.-L. Huang, P. J. Dagdigian, and M. H. Alexander, J. Chem. Phys. **98**, 8484 (1993).